THE JOURNAL OF PHYSICAL CHEMISTRY B

Article

pubs.acs.org/JPCB

# A New Theoretical Approach to Analyze Complex Processes in Cytoskeleton Proteins

Xin Li and Anatoly B. Kolomeisky*

Department of Chemistry and Center for Theoretical Biological Physics, Rice University, Houston, Texas 77005, United States

**ABSTRACT:** Cytoskeleton proteins are filament structures that support a large number of important biological processes. These dynamic biopolymers exist in nonequilibrium conditions stimulated by hydrolysis chemical reactions in their monomers. Current theoretical methods provide a comprehensive picture of biochemical and biophysical processes in cytoskeleton proteins. However, the description is only qualitative under biologically relevant conditions because utilized theoretical mean-field models neglect correlations. We develop a new theoretical method to describe dynamic processes in cytoskeleton proteins that takes into account spatial correlations in the chemical composition of these biopolymers. Our approach is based on analysis of probabilities of different clusters of subunits. It allows us to obtain exact analytical expressions for a variety of dynamic properties of cytoskeleton filaments. By comparing theoretical predictions with Monte Carlo computer simulations, it is shown that our method provides a fully quantitative description of complex dynamic phenomena in cytoskeleton proteins under all conditions.

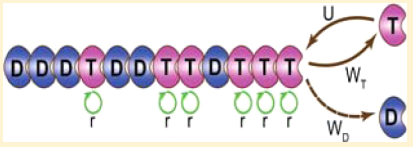




## INTRODUCTION

Cytoskeleton proteins such as microtubules and actin filaments are rigid polymer molecules involved in a variety of fundamental biological processes.[1−3] They play a central role in supporting biological transport, cell motility and division, cytoplasmic organization, signaling, and mechanosensation in cells.[4−6] The structural, biochemical, and dynamic features of cytoskeleton proteins have been extensively studied in recent years.[4,5,7] Advanced experimental methods now allow researchers to look into the assembly and dynamics of cytoskeleton filaments with single-molecule precision and high temporal resolution.[8−10] It was demonstrated that cytoskeleton proteins possess unique biophysical and biochemical properties. However, many of these experimental observations are still not well understood theoretically.

Cytoskeleton proteins can be viewed as complex multifilament structures.[1−3] Actin filaments consist of two polymer chains that are wrapped around each other, producing a right-handed helix. Microtubules typically have 13 parallel protofilaments arranged circumferentially, creating a hollow cylindrical structure. Cytoskeleton proteins are highly dynamic polymers, and they function under nonequilibrium conditions in cells. These conditions are stimulated by energy dissipation produced by hydrolysis processes that are taking place in specific molecules attached to subunits in cytoskeleton proteins. In actin filaments, it is a hydrolysis of adenosine triphosphate (ATP). In microtubules, the hydrolysis of the related monomer-bound molecule guanosine triphosphate (GTP) drives all dynamic processes. Precise molecular mechanisms of hydrolysis in cytoskeleton proteins remain not fully explained despite significant experimental and theoretical efforts.[7,11−13]

It is known that in cells concentrations of free actin monomers and tubulins (cytoskeleton filaments are made of them) are close to the so-called critical concentrations when the average rate of the filament growth is equal to zero. Under these conditions, many dynamic phenomena, including large length fluctuations, treadmilling, and dynamic instability, can be observed in cytoskeleton proteins.[14,15] However, our understanding of underlying mechanisms of these processes is still limited. In recent years, several theoretical approaches have been proposed and applied to explain these fascinating phenomena,[13,16−21] but none of them is able to fully describe them.

Current theoretical methods for investigating dynamic processes in cytoskeleton proteins are based on simplified mean-field models that neglect spatial correlations between different subunits in these filaments.[13,17,20] It gives a reasonable description of many features in actin filaments and microtubules, especially at high concentrations of free actin and tubulin monomers in the solution. However, current methods do not work well at biologically relevant conditions which correspond to small and intermediate concentrations near the critical concentration. Apparently, correlations are significant in this regime. Since most biological phenomena supported by cytoskeleton filaments are taking place under these conditions, it is important to have a theoretical picture that correctly captures microscopic details under these conditions. In this paper, we develop a new theoretical framework for studying dynamic processes in cytoskeleton proteins. It utilizes the analysis of temporal evolution of different clusters of subunits in filaments, and it provides exact analytical expressions for all dynamic properties of these biopolymers. The idea of using clusters has been proposed before,[22,23] but the spatial component of correlations and the dependence on the position in the filament were not included. The main advantage of our

**Received:** January 9, 2014
**Revised:** February 26, 2014
**Published:** February 26, 2014

   dx.doi.org/10.1021/jp500268q | J. Phys. Chem. B 2014, 118, 2966−2972

method is that it accounts for such correlations and provides a fully quantitative description of assembly and growth phenomena in actin filaments and microtubules. Our analytical predictions are tested with Monte Carlo computer simulations.

## THEORETICAL METHOD

It has been argued before that a simplified single-filament picture to describe growth dynamics in cytoskeleton proteins can successfully capture most physical−chemical properties of the system.[20] For this reason, we consider a model of the cytoskeleton filament as shown in Figure 1. Instead of multifilament structure for real microtubules and actin filaments, a single-polymer description is utilized in this model (Figure 1). However, it allows us to develop a quite realistic dynamic picture of processes in cytoskeleton proteins.[20]

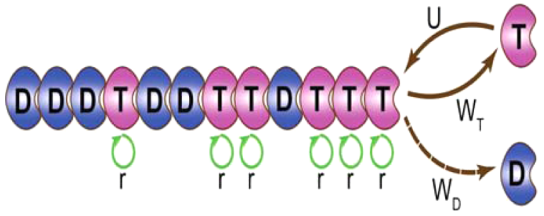


**Figure 1.** Schematic view of a single-filament model for cytoskeleton proteins. The unhydrolyzed subunits bound with GTP(ATP) molecules are indicated by red symbols, while hydrolyzed subunits are shown by blue symbols. $U$ and $W_T$ correspond to the attachment and detachment rates of the T-subunits, respectively. $W_D$ is the detachment rate of the hydrolyzed subunits at the tip of the filament. All T-subunits in the filament can be hydrolyzed with equal probability and with a rate $r$.

Microtubules and actin filaments are formed from the self-assembly of heterodimeric tubulin dimer subunits and actin monomers, respectively. In microtubules, GTP molecules bound to tubulin subunits might hydrolyze, producing guanosine diphosphate (GDP). Similarly, in actin monomers, ATP might hydrolyze to adenosine diphosphate (ADP). The hydrolysis processes in cytoskeleton filaments have several stages, but to simplify calculations, it is frequently considered as a two-state process.[13,20] We also adopt here the two-state picture, and the unhydrolyzed and hydrolyzed monomers are labeled as T-subunits or D-subunits, respectively; see Figure 1. However, our method can be easily extended to include intermediate states of the hydrolysis process.

Both microtubules and actin filaments are polar polymers with different properties for two ends of the filament. One end which has a faster dynamics is called a "plus" end, while the other end is known as a "minus" end. We focus on physical−chemical properties of the "plus" ends of cytoskeleton biopolymers. Each filament can grow by attaching T-subunits to its end with a rate $U = k_{on}C_T$, where $k_{on}$ is the rate constant and $C_T$ is the concentration of free T-subunits in the surrounding solution, which is also assumed to be a constant value. The detachment of the last subunit shortens the filament, and the rate for this process depends on the chemical state of the dissociating subunit. If the filament tip is occupied by a T- or D-subunit, then the corresponding dissociation rates are given by $W_T$ or $W_D$, respectively. The T-subunits in the filament can be hydrolyzed at any time. Currently, the underlying mechanisms for hydrolysis in cytoskeleton filaments are still not well established.[16−18,24−31] Here, we assume that all T-subunits within the filament can be hydrolyzed with equal probability and the hydrolysis rate is equal to $r$, as shown in Figure 1. This is known as a random hydrolysis mechanism.

The main idea of our method is to investigate the dynamics of arbitrary clusters of subunits within the cytoskeleton filament. We define a cluster distribution function $S_n(l, t)$ as a probability to find a cluster of $l$ sites (all T-subunits) starting from the site $n$ (counting from the tip of the polymer) at time $t$ *independently* from the state of all other subunits in the filament. This is different from the probability to have the cluster of *exactly* $l$ T-subunits starting from the site $n$ where sites $n - 1$ and $n + l$ are definitely hydrolyzed. To explain our approach better, we start the analysis with a special case when dissociation rates for hydrolyzed and unhydrolyzed monomers at the tip are the same, $W_T = W_D = W$. It allows us to obtain exact and explicit analytical solutions for cluster distributions at the stationary state, which leads to a full dynamic description of the system. On the basis of these calculations, we continue our derivations for a more realistic general case when T-subunits and D-subunits detach with different rates, $W_T \neq W_D$.

## RESULTS AND DISCUSSION

**Special Case: Equal Detachment Rates for T- and D-Subunits.** For the special case of equal detachment rates from the filament tip, $W_T = W_D = W$, the temporal evolution of the cluster distribution function $S_n(l, t)$ can be described by the following master equations:

$$\frac{dS_n(l,t)}{dt} = US_{n-1}(l,t) + WS_{n+1}(l,t) - (U + W + lr)S_n(l,t) \quad (1)$$

for $n > 1$. The physical meaning of this equation is the following. The first and second terms correspond to a creation of the clusters via shifting the existing segments from the site $n - 1$ or $n + 1$ by adding or removing the subunit at the tip of the polymer, respectively. The third term corresponds to destroying the cluster via addition and removal of the end subunits and also through the hydrolysis process. For the end subunit ($n = 1$), the dynamic rules are different and the corresponding master equations are given by

$$\frac{dS_1(l,t)}{dt} = US_1(l-1,t) + WS_2(l,t) - (U + W + lr)S_1(l,t) \quad (2)$$

for $l > 1$, and the changes in the probability of the cluster $S_1(1, t)$ with $n = 1$ and $l = 1$ are governed by

$$\frac{dS_1(1,t)}{dt} = U + WS_2(1,t) - (U + W + r)S_1(1,t) \quad (3)$$

Importantly, no mean-field assumptions have been made in these equations. Note also that these expressions are written in the system of coordinates where the tip of the filament is always at the origin. One can immediately see the advantage of utilizing clusters, since the spatial correlations are automatically taken into account. Another advantage of this approach is that it recovers existing mean-field theoretical models when only clusters of size one are considered.

To solve the master equations at large times ($t \to \infty$), we look for a solution $S_n(l)$ in the following form:


dx.doi.org/10.1021/jp500268q | J. Phys. Chem. B 2014, 118, 2966−2972

$$S_n(l) = A_l q_l^n \tag{4}$$

where $A_l$ and $q_l$ are unknown parameters that can be obtained by substituting this ansatz into the master equations. First, we substitute eq 4 into eq 1, leading to

$$W q_l^2 - (U + W + lr) q_l + U = 0 \tag{5}$$

The explicit expression for the parameter $q_l$ is then simply given by

$$q_l = \frac{(U + W + lr) - \sqrt{(U + W + lr)^2 - 4UW}}{2W} \tag{6}$$

where it can be shown that the other root of eq 5 is unphysical. For the special case $l = 1$, we have

$$W q_1^2 - (U + W + r) q_1 + U = 0 \tag{7}$$

Interestingly, the parameter $q_1$ here gives the probability that the end subunit of the filament is unhydrolyzed, and it fully agrees with results obtained in the earlier mean-field approach.[18]

Similarly, by substituting eq 4 into eq 3 at stationary state, it can be shown that

$$A_1 W q_1^2 - A_1 (U + W + r) q_1 + U = 0 \tag{8}$$

Then, the solution $A_1 = 1$ can be obtained directly by comparing the above equation with eq 7. From the ansatz for $S_n(l)$, the function $S_1(1)$, which is the probability that the leading subunit is unhydrolyzed, is simply given by $S_1(1) = A_1 q_1 = q_1$. It is fully consistent with the arguments presented above on the physical meaning of the function $q_1$. For parameters $A_l$ with $l > 1$, we use the same strategy and substitute eq 4 into eq 2, yielding

$$U A_{l-1} q_{l-1} + A_l W q_l^2 - A_l (U + W + lr) q_l = 0 \tag{9}$$

Then, one can show that

$$A_l = \prod_{k=1}^{l-1} q_k \tag{10}$$

where eq 5 is employed to derive this result. Finally, the expression for $S_n(l)$ at stationary state can be written as

$$S_n(l) = A_l q_l^n = q_l^{n-1} \prod_{k=1}^{l} q_k \tag{11}$$

where $q_l$ is given explicitly by eq 6. This simple result has a simple physical interpretation. $S_n(l)$ is a product of two terms. The first one, $q_l^{n-1}$, gives the probability to find the cluster at site $n$, while the second, $\prod_{k=1}^{l} q_k$, describes the probability to have $l$ consecutive T-subunits.

The explicit formulas for cluster distributions $S_n(l)$ can be used to obtain all relevant dynamic properties of the filament. Specifically, the function $S_n(1)$ describes a probability density profile of unhydrolyzed T-subunits along the filament. The average number $\langle n \rangle$ of unhydrolyzed monomers in the filament can be easily calculated from

$$\langle n \rangle = \sum_{n=1}^{\infty} S_n(1) \tag{12}$$

producing

$$\langle n \rangle = \frac{U - W - r + \sqrt{(U + W + r)^2 - 4UW}}{2r} \tag{13}$$

As expected, this result suggests that the number of T-subunits in the filament increases for smaller hydrolysis rates.

Another important quantity for actin filaments and microtubules is a cap size which is defined as the average number of unhydrolyzed subunits at the end of the filament (see Figure 1). This cap would help the filament to maintain a stable structure and to prevent it from the fast depolymerization of the exposed hydrolyzed subunits. We can obtain the cap size by introducing a new function $P_l$ from the cluster distributions $S_n(l)$

$$P_l = S_1(l) - S_1(l + 1) \tag{14}$$

It has a physical meaning of probability of having *exactly* $l$ unhydrolyzed subunits at the tip of the filament. It can be shown that

$$P_l = \prod_{k=1}^{l} q_k (1 - q_{l+1}) \tag{15}$$

This result also has a simple physical interpretation that the cluster has $l$ T-subunits, but the $l + 1$-th monomer is already hydrolyzed. Then, the average size $\langle N_{cap} \rangle$ of the cap can be calculated as follows:

$$\langle N_{cap} \rangle = \sum_{l=1}^{\infty} l P_l = \sum_{l=1}^{\infty} \prod_{k=1}^{l} q_k \tag{16}$$

All other dynamic properties of the filament system can be obtained using the same approach.

Previous theoretical methods were also able to calculate various dynamic properties of cytoskeleton proteins.[13,17,20] These models describe quite well the dynamics of actin filaments and microtubules at large concentrations of free monomers in the solution, as found by comparing with Monte Carlo computer simulations. However, all mean-field methods failed to describe the assembly processes quantitatively below and close to the critical concentrations where the growth velocity of the filament vanishes. It suggests that correlations play an important role in controlling dynamic processes in cytoskeleton filaments under these conditions.

To illustrate the method, we test predictions for cluster distribution functions from our analysis and from the simplified mean-field models with Monte Carlo computer simulations. Note that in the mean-field picture the stationary cluster distribution function $S_n(l)$ in our terms can be written as

$$S_n(l) = \prod_{k=n}^{n+l-1} S_k(1) = q_1^{(2n+l-1)l/2} \tag{17}$$

while in our model the expression for $S_n(l)$ is given by eq 11. More specifically, we analyze the stationary cluster distributions $S_1(l)$ and $S_2(l)$ as a function of the cluster size $l$ for microtubules using parameters from Table 1 with the only exception being that the detachment rates are the same, $W_D = W_T = 24\ s^{-1}$. The results are presented in Figure 2. These quantities are calculated for two different free tubulin concentrations. In the first case, we take large $C_T = 20\ \mu M$ (Figure 2A and B), while in the second case $C_T = 5\ \mu M$ close to the critical concentration (~7.5 $\mu M$) is used (Figure 2C and D). One can see that for large free monomer concentrations both theoretical approaches show excellent agreement with


dx.doi.org/10.1021/jp500268q | J. Phys. Chem. B 2014, 118, 2966−2972

**Table 1. Parameters Utilized in Calculations and the Corresponding References**

| parameter | rates | ref |
|---|---|---|
| $k_{on}$, on-rate of T-tubulin dimers (plus end) | 3.2 $\mu M^{-1}$ $s^{-1}$ | 2 |
| $W_T$, off-rate of T-tubulin dimers (plus end) | 24 $s^{-1}$ | 32 |
| $W_D$, off-rate of D-tubulin dimers (plus end) | 290 $s^{-1}$ | 2 |
| $r$, hydrolysis rate | 0.2 $s^{-1}$ | 20 |

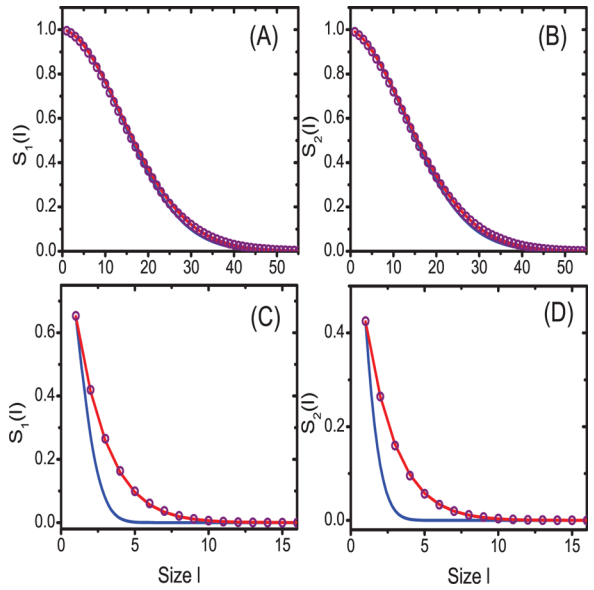


**Figure 2.** The cluster distributions $S_1(l)$ and $S_2(l)$ as a function of the cluster size $l$ for the special case with rates $W_T = W_D = 24$ $s^{-1}$. Parts A and C correspond to the cluster distribution $S_1(l)$. Parts B and D give the cluster distribution $S_2(l)$. The free monomer concentration is 20 $\mu$M for parts A and B and 5 $\mu$M for parts C and D. The red solid lines correspond to the method developed in this work, the blue solid lines are calculated from the previously used mean-field theory,[20] and the open purple circles are from Monte Carlo computer simulations.

results from Monte Carlo computer simulations. However, the predictions from the mean-field model start to deviate at low $C_T$, while our method still shows a perfect agreement with computer simulations under these conditions; see Figure 2C and D.

Different predictions for cluster distribution functions lead to deviations in all dynamic properties of cytoskeleton filaments. For example, in Figure 3A, we compare the results for the cap length at different concentrations of free monomers in the solution. Our approach performs very well at *all* ranges of concentrations, and the results are indistinguishable from computer simulations. At the same time, the simplified mean-field picture shows the deviations below 10 $\mu$M, which is the region around the critical concentration, although they are not large.

**General Case: Detachment Rates for T- and D-Subunits Are Not Equal.** Now we consider a more realistic general case of unequal detachment rates for hydrolyzed and unhydrolyzed subunits at the tip of the filaments. Again, we analyze the temporal evolution of cluster probability functions $S_n(l, t)$ which are governed by master equations

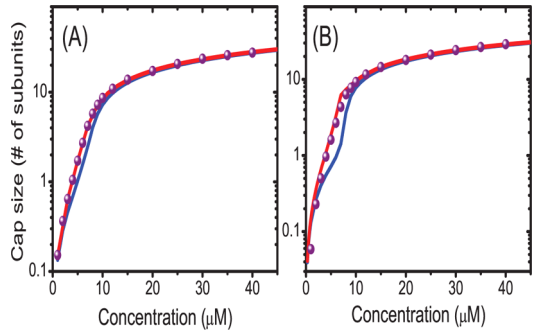


**Figure 3.** The cap size of the filament as a function of T-subunit concentration: (A) for the special case when hydrolyzed and unhydrolyzed subunits detach from the tip of the filament with the same rate $W_T = W_D = 24$ $s^{-1}$; (B) for the general case with the detachment rates for hydrolyzed and unhydrolyzed monomers taken from Table 1. The red solid lines are given by the theory developed in this article, the blue solid lines are obtained from the mean-field theory,[20] and the purple dots are from the Monte Carlo computer simulations.

$$\frac{dS_n(l,t)}{dt} = US_{n-1}(l,t) + W_T S_{n+1}(l,t)S_1(1,t) + W_D S_{n+1}(l,t)(1 - S_1(1,t)) - [U + lr + W_T S_1(1,t) + W_D(1 - S_1(1,t))]S_n(l,t) \quad (18)$$

for $n > 1$. The important observation here is that these equations, in contrast to eq 1, are approximate, since we assumed that the chemical state of the end subunit is independent of the state of any cluster of size $l$ beyond the site $n$. However, by considering clusters, it still takes into account some spatial correlations in comparison with the simplified mean-field approach where the chemical states of *any* two neighboring subunits are assumed always to be independent. For $W_T = W_D$, eq 18 reduces, as expected, to eq 1 and no assumptions are needed.

Similarly to the special case, the dynamic rules change for the end subunit ($n = 1$), and we have the following master equations:

$$\frac{dS_1(l,t)}{dt} = US_1(l-1,t) + W_T S_2(l,t)S_1(1,t) + W_D S_2(l,t)(1 - S_1(1,t)) - (U + W_T + lr)S_1(l,t) \quad (19)$$

for $l > 1$, and for the distribution $S_1(1, t)$ with $n = 1$ and $l = 1$, it can be shown that

$$\frac{dS_1(1,t)}{dt} = U + W_T S_2(1,t)S_1(1,t) + W_D S_2(1,t)(1 - S_1(1,t)) - (U + W + r)S_1(1,t) \quad (20)$$

At stationary state, we use the same ansatz eq 4 for the function $S_n(l)$ in eq 18, and it leads to the following expression:

$$U + W_T q_l^2 A_1 q_1 + W_D q_l^2 (1 - A_1 q_1) - [U + lr + W_T A_1 q_1 + W_D(1 - A_1 q_1)]q_l = 0 \quad (21)$$

Note that here the function $q_l$ depends on the parameters $q_1$ and $A_1$. This equation reduces to eq 5 for the same detachment rates $W_T = W_D$. For the case $l = 1$ from eq 21, we obtain


dx.doi.org/10.1021/jp500268q | J. Phys. Chem. B 2014, 118, 2966−2972

$$U + A_1 W_T q_1^3 + (1 - A_1 q_1) W_D q_1^2 - [U + r + W_T A_1 q_1 + W_D(1 - A_1 q_1)] q_1 = 0 \quad (22)$$

Now, applying the ansatz eq 4 in eq 20 at large times yields another equation

$$U + A_1^2 W_T q_1^3 + (1 - A_1 q_1) A_1 W_D q_1^2 - (U + r + W_T) A_1 q_1 = 0 \quad (23)$$

Comparing eqs 22 and 23, one can find that the simple solution $A_1 = 1$ obtained for the special case of $W_T = W_D$ does not work in the general situation. However, these two algebraic equations can be solved together to determine numerically exactly the unknown parameters $q_1$ and $A_1$. It will provide expressions for parameters $q_l$ from eq 21. However, we also need to determine parameters $A_l$ for $l > 1$. It can be done by substituting eq 4 into eq 19, leading to the following recursion relation:

$$A_l = \lambda_l A_{l-1} q_{l-1} \quad (24)$$

where

$$\lambda_l = \frac{1}{1 - q_l(W_D - W_T)(1 - A_1 q_1)/U} \quad (25)$$

Therefore, the parameter $A_l$ can be described explicitly as

$$A_l = \frac{A_1}{\lambda_1 q_l} \prod_{k=1}^{l} \lambda_k q_k \quad (26)$$

Finally, the general solution for $S_n(l)$ at stationary state can be written in terms of already calculated parameters $q_l$ and $A_l$

$$S_n(l) = A_l q_l^n = \frac{A_1 q_l^{n-1}}{\lambda_1} \prod_{k=1}^{l} \lambda_k q_k \quad (27)$$

These results allow us to obtain all dynamic properties of cytoskeleton filaments, as was described in detail for the special case.

Since our method for the general case of unequal detachment rates is also approximate, it is important to test its predictions. In Figure 4, the stationary cluster distribution functions $S_1(l)$ and $S_2(l)$ as a function of the cluster size $l$ are presented for two different concentrations of free monomers in the solution. Cluster distributions at $C_T = 20$ $\mu$M are shown in Figure 4A and B. This concentration is larger than the critical concentration for this case which is equal to 8.1 $\mu$M. The cluster distributions at $C_T = 5$ $\mu$M are plotted in Figure 4C and D. One can see that both the simplified mean-field and our model give excellent predictions for large concentrations (see Figure 4A and B). However, it should be noted that there are small deviations from simulations for the simplified mean-field model for $S_2(l)$ for clusters larger than $l = 25$, while our method is still very good at all cluster sizes. The picture is very different at small concentrations where the simplified mean-field method fails to properly describe cluster distribution functions, and the performance for $S_2(l)$ is worse than that for $S_1(l)$; see Figure 4C and D. Comparing Figures 2 and 4, we might conclude that for more realistic biological conditions the role of correlations is even stronger than that for the special case. This conclusion can be illustrated by considering the calculated cap sizes for cytoskeleton filaments, as presented in Figure 3. For realistic microtubule parameters (Figure 3B), deviations of the simplified mean-field model near the critical concentrations become significant. At the same time, our method fully accounts for all dynamic behavior under all conditions, suggesting that spatial correlations cannot be ignored.

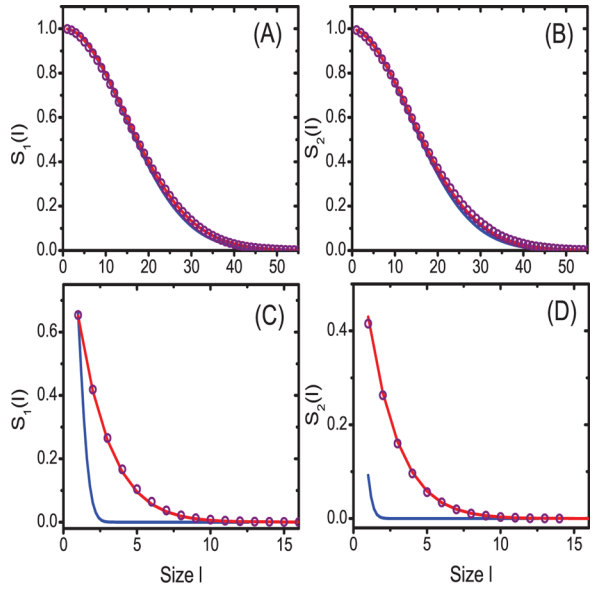


**Figure 4.** The cluster distributions $S_1(l)$ and $S_2(l)$ as a function of the cluster size $l$ for the general case with rates $W_T \neq W_D$ as given in Table 1. Parts A and C correspond to the cluster distribution $S_1(l)$. Parts B and D give the cluster distribution $S_2(l)$. The free T-subunit concentration is equal to 20 $\mu$M for parts A and B, and it is equal to 5 $\mu$M for parts C and D. The red solid lines are obtained from the theoretical approach developed in this work, the blue solid lines correspond to the previously utilized mean-field theory,[20] and the open purple circles are calculated from the Monte Carlo computer simulations.

To analyze the role of correlations in dynamic processes in cytoskeleton proteins, we consider a new function $\tau_{1,2}$ defined as

$$\tau_{1,2} = \frac{S_1(2)}{S_1(1)S_2(1)} \quad (28)$$

It gives a quantitative measure of correlations for the last two subunits in the polymer. The value of $\tau_{1,2}$ should be equal to 1 if there are no correlations between the chemical states of the last two subunits. Deviations from unity will show the degree of correlations in this case. This quantity is presented in Figure 5 for realistic microtubule parameters from Table 1. One can see that correlations disappear above the critical concentration (8.1 $\mu$M), while below the critical concentration they are significant and increase with lowering $C_T$. It explains the success of our method in describing dynamic properties of cytoskeleton proteins because it accounts for spatial correlations between subunits in the polymer.

We can give the following simple arguments for why correlations play an important role under conditions near or below the critical concentration. At large concentrations, the chemical process of attachment of monomers to the filament dominates the process, leading to a large cap of unhydrolyzed T-subunits. It means that most monomers are not hydrolyzed, and its position relative to the tip of the polymer and the chemical state of their neighbors do not affect their fates. This effectively corresponds to the absence of correlations. The situation changes dramatically at the critical concentration and below. Here detachments and hydrolysis are becoming more


dx.doi.org/10.1021/jp500268q | J. Phys. Chem. B 2014, 118, 2966−2972

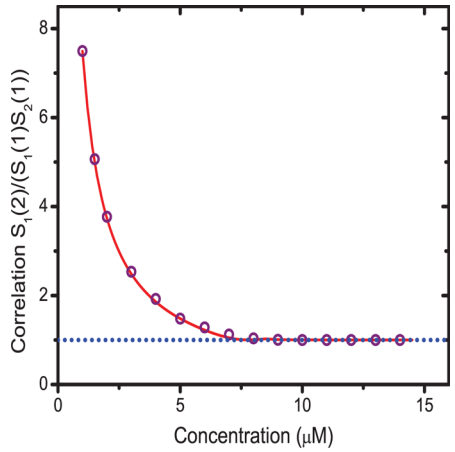


**Figure 5.** The correlation parameter $\tau_{1,2} = S_1(2)/(S_1(1)S_2(1))$ as a function of the free monomer concentration. The red solid line is given by the theory developed in this work, and the open purple circles are obtained from the Monte Carlo computer simulations. The dotted line corresponds to unity.

relevant in comparison to attachments. In this case, the relative position of the subunit and the chemical states of its neighbors are more important, which is a signature of correlations.

## SUMMARY AND CONCLUSIONS

In this work, we developed a new theoretical framework for investigating dynamic processes in cytoskeleton proteins. Our approach is based on analysis of probability distribution functions for clusters of subunits, which leads to a full description of all biophysical and biochemical processes in filaments. The main advantage of the method is the fact that it accounts for spatial correlations between chemical states of different monomers, while still allowing to obtain analytical expressions for all relevant physical−chemical properties of cytoskeleton filaments.

First, the method was developed for the special case of equal detachment rates for hydrolyzed and unhydrolyzed subunits. In this case, the dynamics at stationary state is solved exactly for all range parameters. The predictions fully agree with Monte Carlo computer simulations. The method is extended then to more realistic general cases of unequal detachment rates where an approximate scheme, that still takes into account some correlations, is presented. It is found that this approach again provides a fully quantitative view of all dynamic processes in cytoskeleton filaments, as supported by Monte Carlo computer simulations. In contrast, the widely used simplified mean-field models that neglect correlations cannot properly capture the dynamics of cytoskeleton filaments under conditions near and below the critical concentration, where the average filament growth velocity vanishes, and they can only be used reliably at large concentrations of free monomers in the solution. Finally, it was observed that the correlations influence dynamics of cytoskeleton filaments under conditions near and below the critical concentrations. We presented physical arguments to explain this, suggesting that at these conditions detachments and hydrolysis processes become more prominent, while at large concentrations they do not play any role.

Despite the success of the presented method, it should be noted that it gives an oversimplified picture of complex dynamic processes taking place in cytoskeleton filaments. Our approach obviously omits many important phenomena that should be taken into account. Real actin filaments and microtubules have multifilament structures, and taking this into account significantly complicates calculations for all dynamic properties. We expect that the role of correlations in multifilament proteins could be even more important in comparison with a single-filament polymer because of lateral interactions between subunits from the neighboring protofilaments. In this work, we assumed a random hydrolysis mechanism when the hydrolysis can take place with equal probability at any subunit. There are several proposals arguing that cooperativity might play a stronger role in the hydrolysis in cytoskeleton proteins, and our method can be extended to analyze these possibilities. It will be important also to test our theoretical predictions in more detailed theoretical treatments as well as in experimental studies.

## AUTHOR INFORMATION

### Corresponding Author

*E-mail: tolya@rice.edu. Phone: +1 713 3485672. Fax: +1 713 3485155.

### Notes

The authors declare no competing financial interest.

## ACKNOWLEDGMENTS

The work was supported by a grant from the Welch Foundation (C-1559).

## REFERENCES

(1) Alberts, B.; Johnson, A.; Lewis, J.; Raff, M.; Roberts, K.; Walter, P. *Molecular Biology of the Cell*, 5th ed.; Garland Science: New York, 2007.

(2) Howard, J. *Mechanics of Motor Proteins and the Cytoskeleton*; Sinauer Associates: Sunderland, MA, 2001.

(3) Phillips, R.; Kondev, J.; Theriot, J. *Physical Biology of the Cell*; Garland Science: New York, 2009.

(4) Desai, A.; Mitchison, T. J. Microtubule polymerization dynamics. *Annu. Rev. Cell Dev. Biol.* **1997**, *13*, 83−117.

(5) Pollard, T. D.; Blanchoin, L.; Mullins, R. D. Molecular Mechanisms Controlling Actin Filament Dynamics in Nonmuscle Cells. *Annu. Rev. Biophys. Biomol. Struct.* **2000**, *29*, 545−576.

(6) Bray, D. *Cell Movements: From Molecules to Motility*, 2nd ed.; Garland Publishing: New York, 2001.

(7) Gardner, M. K.; Zanic, M.; Howard, J. Microtubule catastrophe and rescue. *Curr. Opin. Cell Biol.* **2013**, *25*, 14−22.

(8) Schek, H. T.; Hunt, A. J. Micropatterned Structures for Studying the Mechanics of Biological Polymers. *Biomed. Microdevices* **2005**, *7*, 41−46.

(9) Kerssemakers, J. W. J.; Munteanu, E. L.; Laan, L.; Noetzel, T. L.; Janson, M. E.; Dogterom, M. Assembly Dynamics of Microtubules at Molecular Resolution. *Nature* **2006**, *442*, 709−712.

(10) Dimitrov, A.; Quesnoit, M.; Moutel, S.; Cantaloube, I.; Pous, C.; Perez, F. Detection of GTP-Tubulin Conformation in Vivo Reveals a Role for GTP Remnants in Microtubule Rescues. *Science* **2008**, *322*, 1353−1356.

(11) Carlsson, A. E. Actin Dynamics: from Nanoscale to Microscale. *Annu. Rev. Biophys.* **2010**, *39*, 91−110.

(12) Bugyi, B.; Carlier, M. F. Control of Actin Filament Treadmilling in Cell Motility. *Annu. Rev. Biophys.* **2010**, *39*, 449−470.

(13) Li, X.; Kolomeisky, A. B. Theoretical Analysis of Microtubules Dynamics Using a Physical-Chemical Description of Hydrolysis. *J. Phys. Chem. B* **2013**, *117*, 9217−9223.

(14) Fujiwara, I.; Takahashi, S.; Tadakuma, H.; Funatsu, T.; Ishiwata, S. Microscopic Analysis of Polymerization Dynamics with Individual Actin Filaments. *Nat. Cell Biol.* **2002**, *4*, 666−673.

(15) Drechsel, D. N.; Hyman, A. A.; Cobb, M. H.; Kirschner, M. W. Modulation of the Dynamic Instability of Tubulin Assembly by the

Microtubule-Associated Protein Tau. *Mol. Biol. Cell* **1992**, *3*, 1141−1154.
(16) Flyvbjerg, H.; Holy, T. E.; Leibler, S. Stochastic Dynamics of Microtubules: A Model for Caps and Catastrophes. *Phys. Rev. Lett.* **1994**, *73*, 2372−2375.
(17) Vavylonis, D.; Yang, Q.; O'Shaughnessy, B. Actin Polymerization Kinetics, Cap Structure, and Fluctuations. *Proc. Natl. Acad. Sci. U.S.A.* **2005**, *102*, 8543−8548.
(18) Stukalin, E. B.; Kolomeisky, A. B. ATP Hydrolysis Stimulates Large Length Fluctuations in Single Actin Filaments. *Biophys. J.* **2006**, *90*, 2673−2685.
(19) Brun, L.; Rupp, B.; Ward, J. J.; Nedelec, F. A Theory of Microtubule Catastrophes and their Regulation. *Proc. Natl. Acad. Sci. U.S.A.* **2009**, *106*, 21173−21178.
(20) Padinhateeri, R.; Kolomeisky, A. B.; Lacoste, D. Random Hydrolysis Controls the Dynamic Instability of Microtubules. *Biophys. J.* **2012**, *102*, 1274−1283.
(21) Yogurtcu, O. N.; Kim, J. S.; Sun, S. X. A Mechanochemical Model of Actin Filaments. *Biophys. J.* **2012**, *103*, 719−727.
(22) Antal, T.; Krapivsky, P. L.; Redner, S.; Mailman, M.; Chakraborty, B. Dynamics of an Idealized Model of Microtubule Growth and Catastrophe. *Phys. Rev. E* **2007**, *76*, 041907.
(23) Li, X.; Lipowsky, R.; Kierfeld, J. Coupling of Actin Hydrolysis and Polymerization: Reduced Description with Two Nucleotide States. *Europhys. Lett.* **2010**, *89*, 38010.
(24) Blanchoin, L.; Pollard, T. D. Hydrolysis of ATP by Polymerized Actin Depends on the Bound Divalent Cation but Not Profilin. *Biochemistry* **2002**, *41*, 597−602.
(25) VanBuren, V.; Odde, D. J.; Cassimeris, L. Estimates of Lateral and Longitudinal Bond Energies within the Microtubule Lattice. *Proc. Natl. Acad. Sci. U.S.A.* **2002**, *99*, 6035−6040.
(26) Bindschadler, M.; Osborn, E. A.; Dewey, C. F.; McGrath, J. L. A Mechanistic Model of the Actin Cycle. *Biophys. J.* **2004**, *86*, 2720−2739.
(27) Erlenkamper, C.; Kruse, K. Uncorrelated Changes of Subunit Stability can Generate Length-Dependent Disassembly of Treadmilling Filaments. *Phys. Biol.* **2009**, *6*, 046016.
(28) Pantaloni, D.; Hill, T. L.; Carlier, M. F.; Korn, E. D. A Model for Actin Polymerization and the Kinetic Effects of ATP Hydrolysis. *Proc. Natl. Acad. Sci. U.S.A.* **1985**, *82*, 7207−7211.
(29) Pieper, U.; Wegner, A. The End of a Polymerizing Actin Filament Contains Numerous ATP−Subunit Segments That Are Disconnected by ADP−Subunits Resulting from ATP Hydrolysis. *Biochemistry* **1996**, *35*, 4396−4402.
(30) Li, X.; Kierfeld, J.; Lipowsky, R. Actin Polymerization and Depolymerization Coupled to Cooperative Hydrolysis. *Phys. Rev. Lett.* **2009**, *103*, 048102.
(31) Burnett, M. M.; Carlsson, A. E. Quantitative Analysis of Approaches to Measure Cooperative Phosphate Release in Polymerized Actin. *Biophys. J.* **2012**, *103*, 2369−2378.
(32) Janson, M. E.; de Dood, M. E.; Dogterom, M. Dynamic Instability of Microtubules is Regulated by Force. *J. Cell Biol.* **2003**, *161*, 1029−1034.